



Contents lists available at ScienceDirect

Arabian Journal of Chemistry

journal homepage: www.ksu.edu.sa

Construction of macromolecular structure in KunNing coal and analysis of Macro-Micro oxidation characteristics

Dongjie Hu^{*}, Zongxiang Li, Yu Liu, Lin Li

College of Safety Science and Engineering, Liaoning Technical University, Liaoning 123000, China

Key Laboratory of Mine Thermodynamic Disasters and Control of Ministry of Education, Liaoning Technical University, Liaoning 123000, China

ARTICLE INFO

Keywords:

Enclosed coal oxidation test
Oxidation heat release intensity
Reaction kinetics
Indicator gas molecule traceback
Active groups

ABSTRACT

To explore the macro–micro coal oxidation characteristics for the purpose of preventing coal spontaneous combustion and achieving efficient coal conversion and utilization, the enclosed coal oxidation characteristics of KunNing coal sample (KN) under 25–70 °C were investigated. KN coal molecular models were constructed based on analysis and testing results of X-ray Photoelectron Spectroscopy (XPS), Carbon-13 Nuclear Magnetic Resonance Spectroscopy (¹³C NMR), Fourier Transform Infrared Spectroscopy (FTIR) and other techniques. The pyrolysis processes of coal-oxygen reaction systems with different oxygen contents were simulated using ReaxFF force field. The results show that the oxygen consumption rate, CO release rate, CO₂ release rate and oxidation heat release intensity of coal increase exponentially with rising temperature. The ratio of aromatic bridge carbon to peripheral carbon in KN coal molecular structure is 0.08, and the molecular formula is C₁₄₉H₇₆O₁₅N₂S₂. In the later stage of the experimental and molecular dynamics simulation processes, the CO content decreased while the growth rate of CO₂ increased. Different indicator gases exhibit varied responses to oxygen content. The C-atom labeling and traceback results for the four indicator gas molecules demonstrate that CO₂ mainly comes from aldehyde, hydroxyl, carboxyl and methoxy groups in coal molecules, CO is primarily generated from esters, phenols, carbonyls, C₂H₂ is predominantly derived from ring-opening and cracking of cycloalkanes, and the source of C₂H₄ is related to cycloalkanes and alcohols.

1. Introduction

Coal spontaneous combustion can lead to fires and explosions, endangering life safety, causing resource waste, and producing large amounts of hazardous gases that contaminate the environment (Liang et al., 2016; Zhang et al., 2015; Onifade and Genc, 2020). Accurately depicting coal molecular composition and structure, thoroughly revealing the reaction mechanisms of different structural units under low-temperature oxidation conditions, and exploring the generation and conversion laws of indicator gases, are the keys to improving cognition on coal spontaneous combustion mechanisms and guiding efficient coal utilization and conversion (Jiang et al., 2019; Bhoi et al., 2014; Zeng et al., 2018).

Utilizing modern testing techniques, such as X-ray Photoelectron Spectroscopy (XPS), Carbon-13 Nuclear Magnetic Resonance Spectroscopy (¹³C NMR), Fourier Transform Infrared Spectroscopy (FTIR), etc., to study coal molecular structure is a common approach adopted by

scholars, and over a hundred coal molecular models have been constructed (Shinn, 1996; Wisler, 1984; Given, 1959). Studying the characteristics and laws of chemical reactions, intermolecular interactions, structural evolutions, product formations, etc. of coal during low-temperature oxidation and combustion from a molecular perspective has become an important way to enrich the mechanisms of coal spontaneous combustion (Mathews et al., 2011; Sen and Dash, 2020). Zhan (Zhan et al., 2014) obtained the initial generation pathways of CO, CO₂ and CH₄ in the initial pyrolysis mechanisms of bituminous coal, and proposed that C₉H₉O radical is an important structure during pyrolysis. Zhang (Zhang et al., 2014) quantitatively derived the effects of humidity and temperature on coal methane adsorption and coal swelling mechanisms from a microscopic perspective through Monte Carlo (MC) and molecular dynamics (MD) simulations. Zheng (Zheng et al., 2013) simulated the pyrolysis process of bituminous coal using ReaxFF molecular dynamics simulation, and obtained the generation sequence of indicator gases which is consistent with the experimentally determined

Peer review under responsibility of King Saud University. Production and hosting by Elsevier.

^{*} Corresponding author at: College of Safety Science and Engineering, Liaoning Technical University, Liaoning 123000, China.

E-mail addresses: djhu0418@gmail.com (D. Hu), lizz6211@163.com (Z. Li).

<https://doi.org/10.1016/j.arabjc.2023.105499>

Received 19 October 2023; Accepted 26 November 2023

Available online 29 November 2023

1878-5352/© 2023 The Author(s). Published by Elsevier B.V. on behalf of King Saud University. This is an open access article under the CC BY-NC-ND license (<http://creativecommons.org/licenses/by-nc-nd/4.0/>).

Table 1
Proximate and ultimate analysis.

Proximate analysis (%)				Elemental analysis (%)				
Moisture	Ash	Volatile	Fixed carbon	C	H	O	N	S
0.99	8.31	9.16	81.54	81.97	3.49	10.94	1.22	2.38

Table 2
Atomic ratio of coal sample (based on C element).

Coal sample	H/C	O/C	N/C	S/C
KN	0.5109	0.1001	0.0128	0.0109

laws. Long (Long et al., 2021) studied the microscopic mechanisms of loading, adsorption and diffusion of CH₄, CO₂ and N₂ gases in coal and the quantitative relationship between coal pore size distribution using Monte Carlo and molecular dynamics simulations. Gao (Gao et al., 2018) employed ReaxFF simulation and found that the main reaction pathways for generating CO₂, H₂O, CH₄ and H₂ during Fugu coal pyrolysis are closely related to carboxyl and methoxy groups. The above studies investigated the interactions and chemical reactions between coal and gas molecules from a microscopic perspective, and the conclusions are of great significance for enriching the mechanisms of coal spontaneous combustion and improving coal conversion and utilization efficiency. However, different types of coal exhibit variations in their physico-chemical properties, which inevitably leads to differences in their molecular structures. Therefore, based on the research conducted by the aforementioned scholars, it is necessary to establish a molecular model for Kunming mine coal and investigate its chemical reaction characteristics.

The KunNing coal type belongs to bituminous coal, which contains a carbon content of 75 % to 90 %, an oxygen content of 10 % to 15 %, and relatively low levels of ash and moisture content. In order to explore the oxidation characteristics of KunNing coal (KN), self-developed enclosed coal oxidation experiments were used to investigate the oxygen consumption, variation laws of generated CO and CO₂ gas concentrations, oxidation heat release intensity and other macroscopic oxidation characteristics of KN coal at 25, 30, 35, 40, 45, 50, 55, 60, 65, 70 °C, respectively. The molecular structure was studied using industrial analysis, elemental analysis, XPS, ¹³C NMR and FTIR from a microscopic perspective, based on which the molecular plane structure model was constructed (Ding et al., 2023; Gao, 2021; Meng et al., 2018). ReaxFF pyrolysis simulation was utilized to analyze the pyrolysis processes of coal-oxygen reaction systems with different oxygen contents, obtaining the molecular structure of KN coal and the initial positions of carbon atoms in CO, CO₂, C₂H₄, C₂H₂ and other indicator gas molecules in the coal molecules (initial structures) as well as the generation pathways of indicator gases. This study will contribute to understanding the oxidation characteristics of KN coal from both macroscopic and microscopic perspectives, and provide theoretical guidance for its coal spontaneous

combustion prevention and control techniques.

2. Experimental and analytical methods

2.1. Coal sample preparation and proximate/ultimate analyses

The raw bituminous coal collected from KunNing Mine in JinZhong City, Shanxi Province was sealed and transported to the laboratory. It was then crushed and sieved below 200 mesh under nitrogen atmosphere to obtain the coal sample (named KN) for subsequent experiments. The KN coal sample was analyzed for proximate and ultimate analyses following Chinese National Standards GB/T 212–2008 and GB/T 31391–2015, using 5E-MAG6600B industrial analyzer manufactured by Jiaozuo Hua coal Mining Equipment Co., Ltd. in China and Vario EL elemental analyzer produced by Elementar Group in Germany, respectively. The results are shown in Table 1. Based on the elemental analysis results in Table 1, the atomic ratios referenced to carbon were calculated as shown in Table 2.

2.2. XPS analysis

X-ray photoelectron spectroscopy (XPS) was performed on a Thermo Fisher Scientific ESCALAB Xi + spectrometer with Al K α radiation ($h\nu = 1486.6$ eV) as the excitation source under ultra-high vacuum around 8×10^{-10} Pa. The signal was accumulated for 10 cycles. The passing energy was 100 eV for survey scan and 30 eV for narrow scan with a step size of 0.05 eV and dwell time of 40–50 ms. All binding energies were referenced to C 1 s at 284.80 eV.

2.3. ¹³C NMR analysis

A 400 MHz Bruker nuclear magnetic resonance spectrometer with a resolution of 4.0 mm was used for ¹³C NMR measurements, equipped with a double resonance MAS probe with a rotor spinning speed of 10 kHz. The pulse width was 4 μ s with a pulse delay time of 1 s and contact time of 2 ms. The number of scans was 10000. Carbon atomic information was probed following SY/T 5777–1995.

2.4. FTIR analysis

Fourier transform infrared spectra were collected on a Thermo Fisher Scientific Nicolet iS10 spectrometer with a resolution of 0.5–1 cm⁻¹ over a scanning range of 4000–400 cm⁻¹ and 32 scans. The coal sample

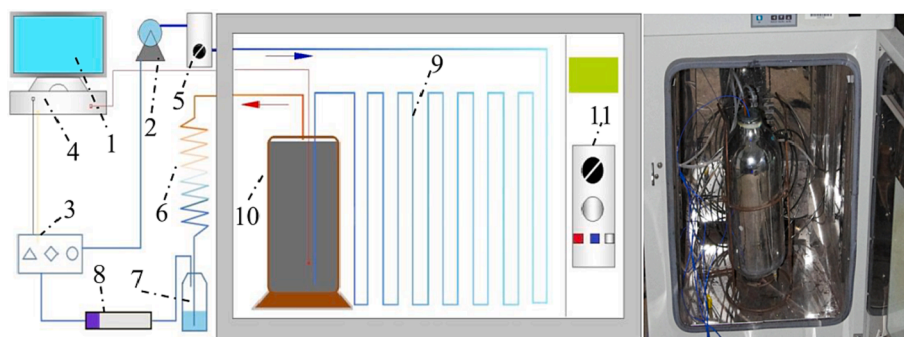


Fig. 1. Schematic of sealed oxygen consumption experimental device.

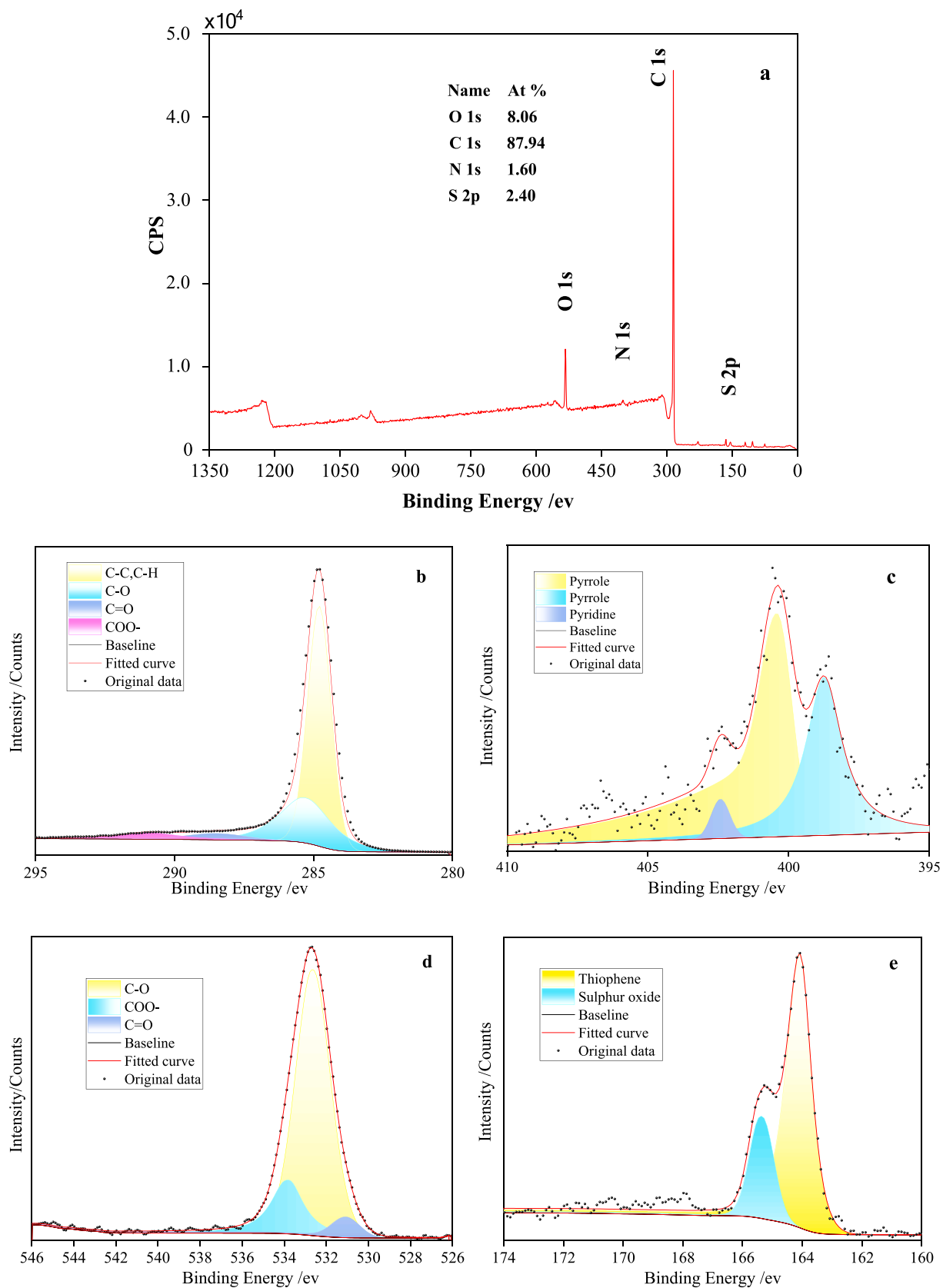


Fig. 2. XPS spectra of the KN coal sample (a - survey; b - C 1 s; c - N 1 s; d - O 1 s; e - S 2p).

Table 3
Attribution summary of XPS binding energies for the KN coal sample.

Figure	Number	Peak position /eV	FWHM /eV	Area	Relative area /%	Attribution
a/C 1 s	1	284.80	1.12	186763.28	64.50	C–C/C–H
	2	285.29	2.19	77120.75	26.64	C–O
	3	288.53	2.50	10901.80	3.77	COO–
	4	290.95	2.49	14669.95	5.08	C = O
b/N 1 s	1	398.74	1.56	3189.38	36.61	Pyrrrole
	2	400.43	1.52	5226.01	60.04	Pyrrrole
	3	402.42	0.79	291.46	3.35	Pyridine
c/O 1 s	1	531.09	1.59	4983.18	7.14	COO–
	2	532.64	1.96	52206.05	74.90	C–O
	3	533.79	1.81	12503.81	17.95	C = O
d/S 2p	1	164.11	0.95	3736.89	61.48	Thiophene
	2	165.32	1.02	2339.87	38.52	Suiphur oxide

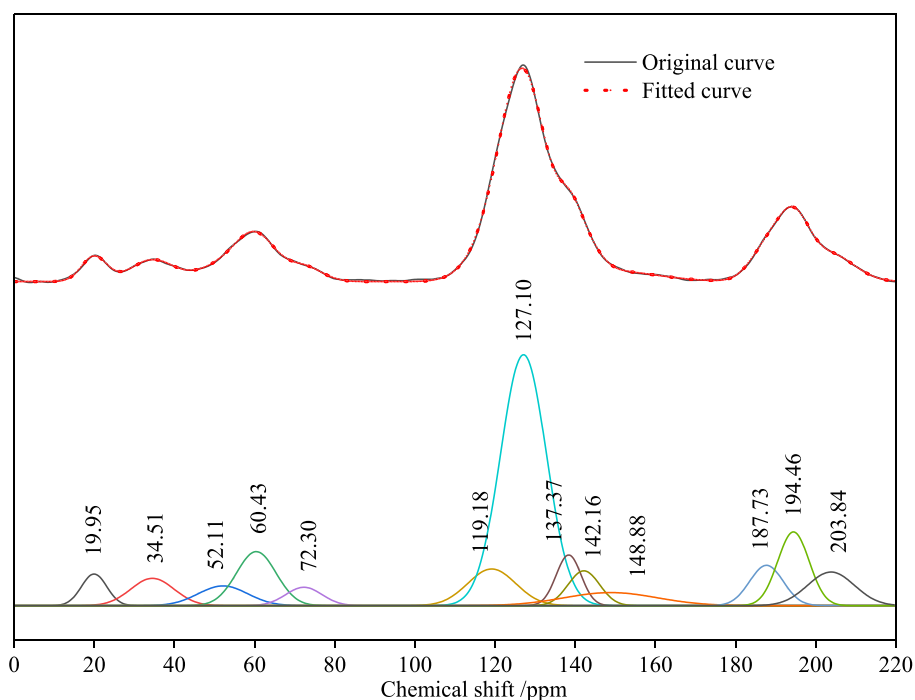


Fig. 3. Experimental and fitted ^{13}C NMR spectra of the coal sample.

was mixed and ground thoroughly with KBr at 1:100 prior to measurement.

2.5. Enclosed coal oxidation experiments

The enclosed coal oxidation experimental setup was independently developed and designed by Professor Li Zongxiang from Liaoning Technical University (Li et al., 2017; Hu and Li, 2022). The schematic diagram of the experimental assembly is illustrated in Fig. 1, which includes: 1) computer, 2) gas pump, 3) gas concentration sensor, 4) data collector, 5) flow meter, 6) condensing tube, 7) collecting bottle, 8) drying tube, 9) preheating pipeline, 10) coal container, and 11) thermostatic oven.

The experimental procedure is as follows: 2.0 kg of crushed coal with a particle size of 0.4–2.4 mm was loaded into the coal container. Gas lines were disconnected 10 mins prior to the test for flushing to eliminate interferences. After reconnecting the setup and ensuring no gas leaks, the thermostatic oven was run to set temperatures of 25, 30, 35, 40, 45, 50, 55, 60, 65, 70 °C for 10 tests. O_2 , CO and CO_2 concentration data were recorded by data acquisition software until the O_2 curve flattened.

2.6. Coal molecular modeling and ReaxFF pyrolysis simulation

Coal macromolecule construction. Based on elemental analysis, FTIR, XPS and ^{13}C NMR results, the coal molecular structure was built in Material Studio and geometry optimized in the Dreiding force field using the Forcite module with Fine quality.

Construction of coal-oxygen mixed systems. The mixed systems containing coal molecules and O_2 were constructed in Amorphous Cell module under 0.5 g/m^3 density (Feng et al., 2019; Zhang, 2022). NPT (constant pressure/temperature) ensemble was employed for density optimization with 30 frames. The lowest energy frame was taken and annealed 30 cycles from 300 to 1000 K under NVE (microcanonical ensemble) using the Anneal module in Forcite to get the optimized lowest energy model.

ReaxFF pyrolysis simulation. The constructed mixed systems were simulated using ReaxFF reactive force field in LAMMPS package. The dynamics calculations were performed under 3D periodic boundary conditions using force field parameters containing C/H/O/N/S/Na elements. The simulation was carried out in the NVE ensemble using the REAX/C computational module, with a time step of 0.2 fs and heating rate of 5 K/ps from 300 to 5000 K (Liu et al.,).

Table 4
Fitted ^{13}C NMR spectral data of the coal sample.

Number	Chemical shift /ppm	Peak type	Peak width	Area	Relative area /%	Attribution
1	19.95	Gaussian	7.42	3.71 $\times 10^8$	2.88	Benzylic carbon
2	34.51	Gaussian	12.72	5.50 $\times 10^8$	4.26	Methylenic carbon
3	52.11	Gaussian	14.52	4.54 $\times 10^8$	3.52	Quaternary and secondary methyl carbon
4	60.43	Gaussian	11.63	9.92 $\times 10^8$	7.69	Methoxy/oxygen-substituted methylene carbon
5	72.30	Gaussian	10.64	3.10 $\times 10^8$	2.40	Oxygen-substituted aliphatic carbon in rings
6	119.18	Gaussian	14.11	8.18 $\times 10^8$	6.34	Protonated aromatic carbon
7	127.10	Gaussian	13.44	5.32 $\times 10^9$	41.23	
8	137.37	Gaussian	7.31	5.85 $\times 10^8$	4.54	Bridging aromatic carbon
9	142.16	Gaussian	9.23	5.08 $\times 10^8$	3.94	Aliphatic carbon attached to aromatic ring
10	148.88	Gaussian	27.36	5.67 $\times 10^8$	4.39	Oxygen-substituted aromatic carbon
11	187.73	Gaussian	9.83	6.26 $\times 10^8$	4.85	Carboxyl carbon
12	194.46	Gaussian	9.20	1.07 $\times 10^9$	8.30	Carbonyl carbon
13	203.84	Gaussian	13.77	7.31 $\times 10^8$	5.67	

3. Results and discussion

3.1. XPS analysis

X-ray photoelectron spectroscopy (XPS) can accurately determine the characteristics of organic functional groups in the 2–5 nm surface molecular layer of coal by measuring the binding energies of photoelectrons from different elements and valence states. The survey spectrum along with C 1 s, N 1 s, O 1 s, S 2p deconvoluted peaks of the KN coal sample are displayed in Fig. 2. The attribution summary of binding energies for quantitative analysis of functional group types and quantities is listed in Table 3.

As shown in Fig. 2 and Table 1, the main components of the coal

Table 5
Structural parameters of carbon species in the coal sample (%).

Coal Sample	f_{al}^f	f_{al}^H	f_{al}^O	f_{al}	f_a^C	f_a	f_a	f_a^H	f_a^N	f_a^S	f_a^B	f_a^P
KN	2.88	15.47	2.40	20.75	13.97	60.44	74.41	47.57	12.87	3.94	4.54	4.39

sample are C and O-containing functional groups and structures, while N and S-containing groups are relatively less. In the C 1 s binding energy region (Fig. 2b), there are 4 fitted peaks attributed to C–H/C–C, C–O, C = O and COO–, among which C–H/C–C and C–O are predominant with area percentages of 64.50 % and 26.64 %, respectively. C = O and COO– contents are lower, consistent with the O 1 s deconvolution results in Fig. 2d, where O atoms mainly exist as C–O, C = O and COO–, with C–O accounting for 74.90 %. As displayed in Fig. 2c, the N 1 s region contains 3 peaks, attributed to Pyrrole and Pyridine, with Pyrrole as the major form. Fig. 2e shows 2 peaks for S 2p, with peak 1 (61.48 %) belonging to thiophene organic sulfur structure and the other peak assigned to inorganic sulfates.

3.2. ^{13}C NMR analysis

^{13}C NMR spectroscopy can sensitively determine the carbon existence forms in coal molecules, thereby reflecting the approximate structure of coal molecular backbone. The ^{13}C NMR spectrum is divided into four chemical shift regions based on the types of chemical functionalities: 0–60 ppm - aliphatic carbon, 60–90 ppm - ether oxygen, 90–165 ppm - aromatic carbon, and ~ 200 ppm - carbonyl peak. Fitting of the processed data yielded 13 peaks in the ^{13}C NMR spectrum of the KN coal sample, as displayed in Fig. 3, with detailed parameters listed in Table 4.

Protonated aromatic carbons account for 47.57 % of the total peak area, indicating the predominant basic structure of protonated aromatic carbons in KN coal molecular skeleton, while other carbon types (like bridgehead aromatic, branched aromatic, aromatic methyl, oxygen-substituted aromatic carbons, etc.) are present in smaller quantities.

According to chemical shift regions and analysis of Table 4, the structural parameters involving 12 carbon species in the molecular backbone were obtained as shown in Table 5 (Yao et al., 2003; Solum et al., 1989).

The mean aromatic condensation degree X_{BP} was calculated using Eq. (1).

$$X_{BP} = f_a^B / (f_a^H + f_a^P + f_a^S) \quad (1)$$

The obtained X_{BP} value for KN coal sample is 0.08, which can be used to estimate the number and condensation degree of benzene rings as well as the aromatic ring size.

3.3. FTIR analysis

FTIR spectroscopy is an important technique to determine the connectivity modes of aliphatic structures, oxygen-containing functionalities, aromatic structures and other cycloalkane structures in coal. Fig. 4 illustrates the fitted FTIR spectrum of the KN coal sample, which can be primarily categorized into 4 regions (Gao et al., 2018; Gao, 2021; Zhang, 2022): 900–700 cm^{-1} ; 1800–1000 cm^{-1} , 3000–2800 cm^{-1} and 3600–3000 cm^{-1} . The peaks from 900 – 700 cm^{-1} and 1800–1000 cm^{-1} correspond to various aromatic hydrocarbon structures, including 1,2-disubstituted, 1,2,4/1,2,3,4-trisubstituted aromatics and C–C vibrations in aromatics.

The vibration of carbonyl groups (C = O) in the 1800–1000 cm^{-1} range likely indicates the presence of some carbonyl-containing compounds. The 3000–2800 cm^{-1} region represents aliphatic CH and CH₂ vibrations, suggesting aliphatic compounds in coal. C–O vibrations in 1800–1000 cm^{-1} imply coal may contain phenols, alcohols, ethers, esters and other functionalities. Further FTIR analysis parameters of the

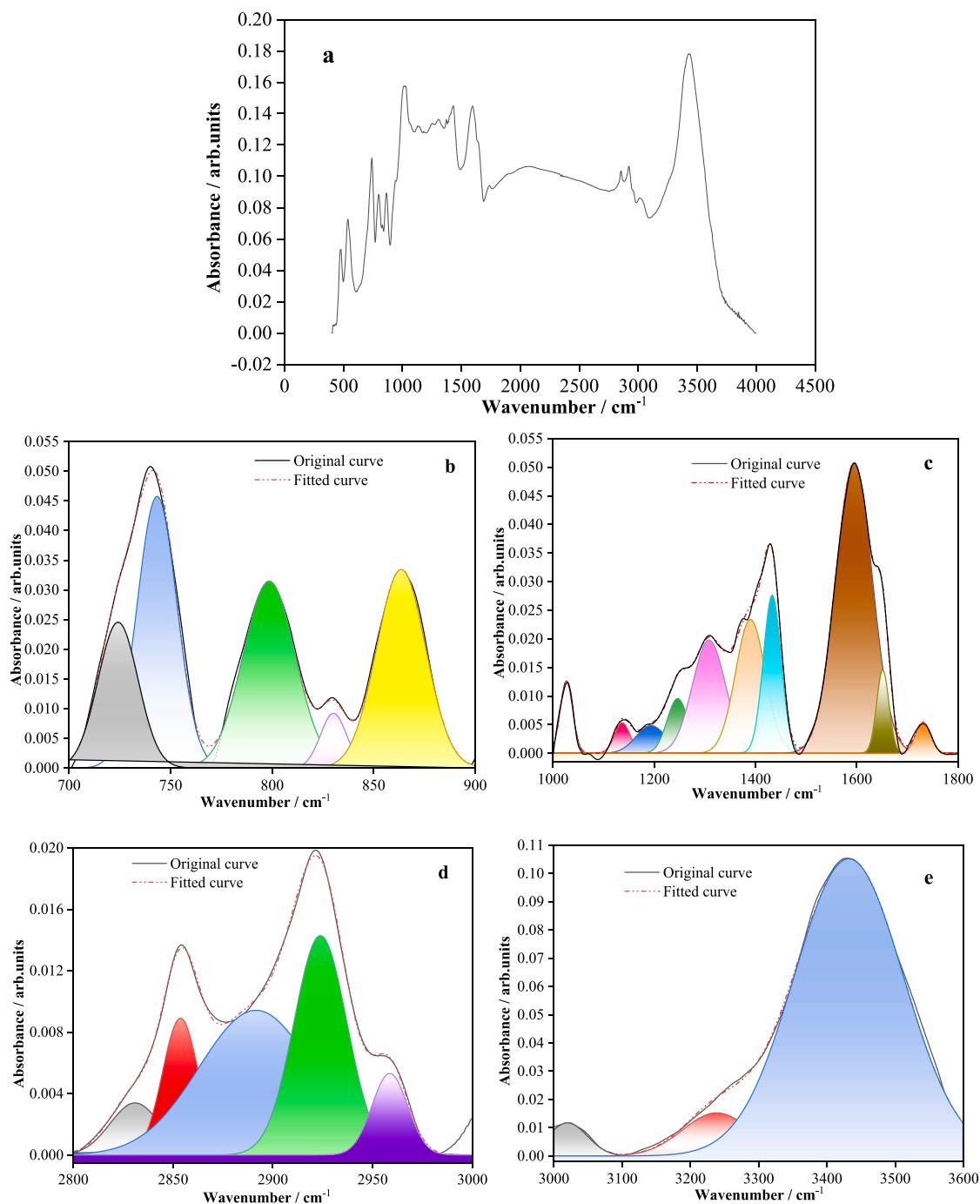


Fig. 4. Fitted FTIR spectrum of the coal sample (a is the full spectrum curve).

KN coal sample are listed in Table 6.

3.4. Construction of coal macromolecular models

Elucidating coal macromolecular structures is crucial for investigating the physicochemical properties of coal at the microscopic level, providing access to transition states, free radicals, bond energies and many other results hard to obtain from macroscopic experiments via quantum mechanical molecular simulations.

According to the elemental ratios in Table 2, assuming the number of C atoms in the coal molecule is x , the molecular formula of KN coal sample can be written as $C_xH_{0.5109x}O_{0.1001x}N_{0.0128x}S_{0.0109x}$. Relevant research shows the molecular weight of coal is around 2000–3000, and

the atomic numbers should be integers. Hence, the molecular formula of KN coal was determined using Eq. (2) by taking $x = 149$, giving $C_{149}H_{76}O_{15}N_2S_2$ and $M = 2204$.

$$M_{KN} = 12x + 0.5109x + 16 \times 0.1001x + 14 \times 0.0128x + 32 \times 0.0109x \quad (2)$$

The types and numbers of carbon atoms were calculated based on the ^{13}C NMR results (Gao, 2021), including protonated aromatic (F_a^H), bridgehead aromatic (F_a^B), branched aromatic (F_a^S), oxygen-substituted aromatic (F_a^O), total aromatic (F_a^T), carbonyl (F_a^C) and aliphatic (F_{Al}) carbons, as listed in Table 7.

3.4.1. Aromatic structures

The C content in KN coal is 81.97 %, and the X_{BP} ratio between

Table 6
FTIR absorption peak parameters of the KN coal sample.

Figure	Number	Peak position /cm ⁻¹	Peak width /cm ⁻¹	Peak type	Area	Area /%	Attribution
a	1	724.14	23.26	Gaussian	0.60	15.49	1,3-disubstituted aromatic CH
	2	743.35	22.97	Gaussian	1.12	28.74	1,2-disubstituted aromatic CH
	3	798.54	30.20	Gaussian	1.01	25.99	1,2,4/1,2,3,4-tetrasubstituted aromatic CH
	4	830.25	15.16	Gaussian	0.15	3.82	1,4-disubstituted aromatic CH
	5	863.55	28.41	Gaussian	1.01	25.96	1,2,4/1,2,3,4,5-pentasubstituted aromatic CH
b	1	1026.58	28.98	Gaussian	0.38	3.41	Ash
	2	1136.78	36.03	Gaussian	0.20	1.82	C-O in phenols, alcohols, ethers, esters
	3	1193.54	69.52	Gaussian	0.36	3.19	
	4	1246.28	48.88	Gaussian	0.50	4.43	
	5	1308.27	77.01	Gaussian	1.62	14.42	
	6	1390.18	69.17	Gaussian	1.72	15.32	-CH ₃ symmetric deformation vibration
	7	1433.21	41.40	Gaussian	1.22	10.82	-CH ₂ and -CH ₃ , inorganic carbonates
	8	1594.96	85.18	Gaussian	4.60	40.88	Aromatic C-C
	9	1651.66	28.51	Gaussian	0.44	3.92	Carbonyl; -O-substituted aromatic C = C
	10	1731.19	34.59	Gaussian	0.20	1.78	Aliphatic C = O
c	1	2830.92	29.32	Gaussian	0.11	6.73	Aliphatic CH ₂ symmetric stretching
	2	2853.71	21.12	Gaussian	0.20	12.73	Aliphatic CH ₃ symmetric stretching
	3	2891.56	67.25	Gaussian	0.67	42.85	Aliphatic CH asymmetric stretching
	4	2923.84	31.17	Gaussian	0.47	30.13	Aliphatic CH ₂ asymmetric stretching
	5	2958.61	21.01	Gaussian	0.12	7.56	Aliphatic CH ₃ asymmetric stretching
d	1	3019.96	67.99	Gaussian	0.85	3.57	Aromatic CH stretching
	2	3238.39	117.63	Gaussian	1.91	8.01	Hydrogen-bonded -OH, -NH; phenols
	3	3431.95	188.10	Gaussian	21.06	88.42	Hydroxyl

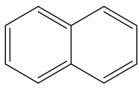
Table 7
Numbers of different carbon species in KN coal sample.

Parameter	$F_a^{H_i}$	$F_a^{P_i}$	$F_a^{S_i}$	$F_a^{P_i}$	$F_a^{I_i}$	$F_a^{C_i}$	F_{AL}
Number	71	7	6	6	90	21	31

Table 8
Aliphatic carbon structural parameters in KN coal molecular structure.

Coal sample	$H_a / \%$	C_n	$C_m / \%$	$\epsilon / \%$	CH ₂ :CH ₃
KN	11.17	0.50	19.18	17.30	1.48

Table 9
Aromatic structural units in the coal sample.

Structure type	X_{BP}	Number	Structure type	X_{BP}	Number
	0	0		0	4
	0	2		0.25	5
	0	2			

aromatic bridge and peripheral carbons is 0.08. This is close to 0 for benzene but lower than 0.25 for naphthalene. The XBP values for anthracene/phenanthrene, tetracene and pentacene are 0.4, 0.5 and 0.57, respectively (Trehwella et al., 1986; Zhou, 2008). Therefore, the molecular structure of KN coal is primarily composed of benzene and naphthalene units, with negligible anthracene/phenanthrene contents.

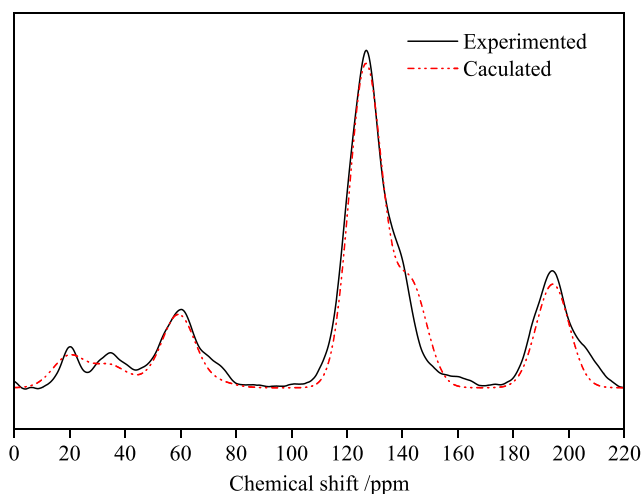


Fig. 5. Comparison of experimental and model ¹³C NMR spectra.

The XPS results also indicate small amounts of pyrrole and thiophene structures present in the macromolecules.

3.4.2. Aliphatic carbon structures

For aliphatic carbons, the carbon atoms mainly exist in the form of aliphatic side chains, cycloalkanes and hydrogenated aromatic rings. Combined with the FTIR results of KN coal sample, its aliphatic structures are present primarily as alkyl side chains and cycloalkanes. The ¹³C NMR data also show the presence of oxygen-substituted aliphatic carbons in the molecular structure (Ding et al., 2023; Gao, 2021; Zhang, 2022). The calculated aromaticity H_a , average number of carbons per methylene chain C_n , degree of alkyl chain branching C_m , aromatic substitution degree ϵ , and CH₂:CH₃ ratio based on ¹³C NMR results are listed in Table 8.

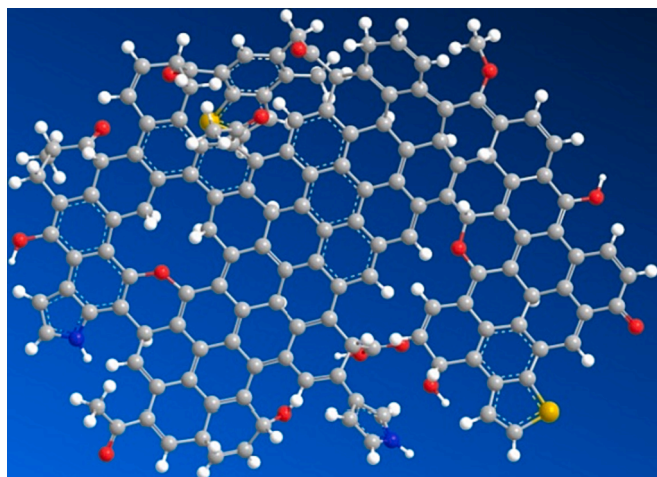


Fig. 6. Molecular structure model of KN coal.

3.4.3. Other heteroatom types

Elemental analysis indicates small amounts of N and S in the KN coal sample. According to the XPS results, N in the form of pyrrole rings

accounts for over 90 % of the total N content. Without considering inorganic sulfur, S elements in coal mainly exist as thiophene, thiol, sulfide, disulfide and thioxanthone (Liu, 2019). The calculated N and S atomic numbers in the KN coal molecule are both 2. Combined with the XPS data, the molecular structure of KN coal is determined to contain 2 pyrrole and 2 thiophene units.

3.4.4. Coal macromolecular model

Based on the above analysis and Table 7, the molecular structure of KN coal is primarily composed of benzene and naphthalene units, with negligible anthracene/phenanthrene contents, as well as small amounts of pyrrole and thiophene structures. The aromatic unit types and numbers are listed in Table 9.

The coal molecular structure was constructed using MS software. The ^{13}C NMR spectrum of this macromolecular model was calculated using MestReNova and compared with the experimental spectrum in Fig. 2. The molecular structure was adjusted to match the experimental NMR results as much as possible, as shown in Fig. 5. Geometry optimization was then performed in the Dreiding force field using the Forcite module in MS. The final optimized macromolecular structure model of KN coal is displayed in Fig. 6.

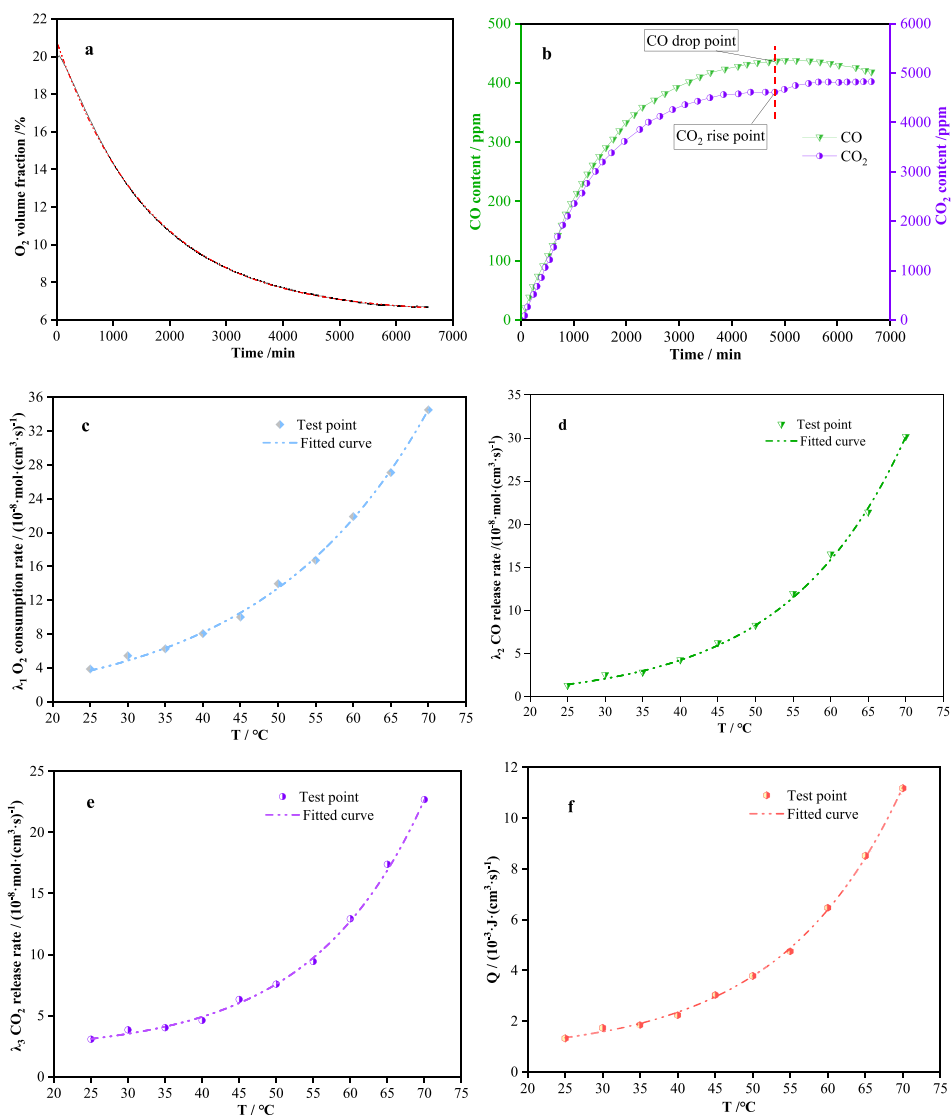


Fig. 7. Enclosed coal oxidation test results.

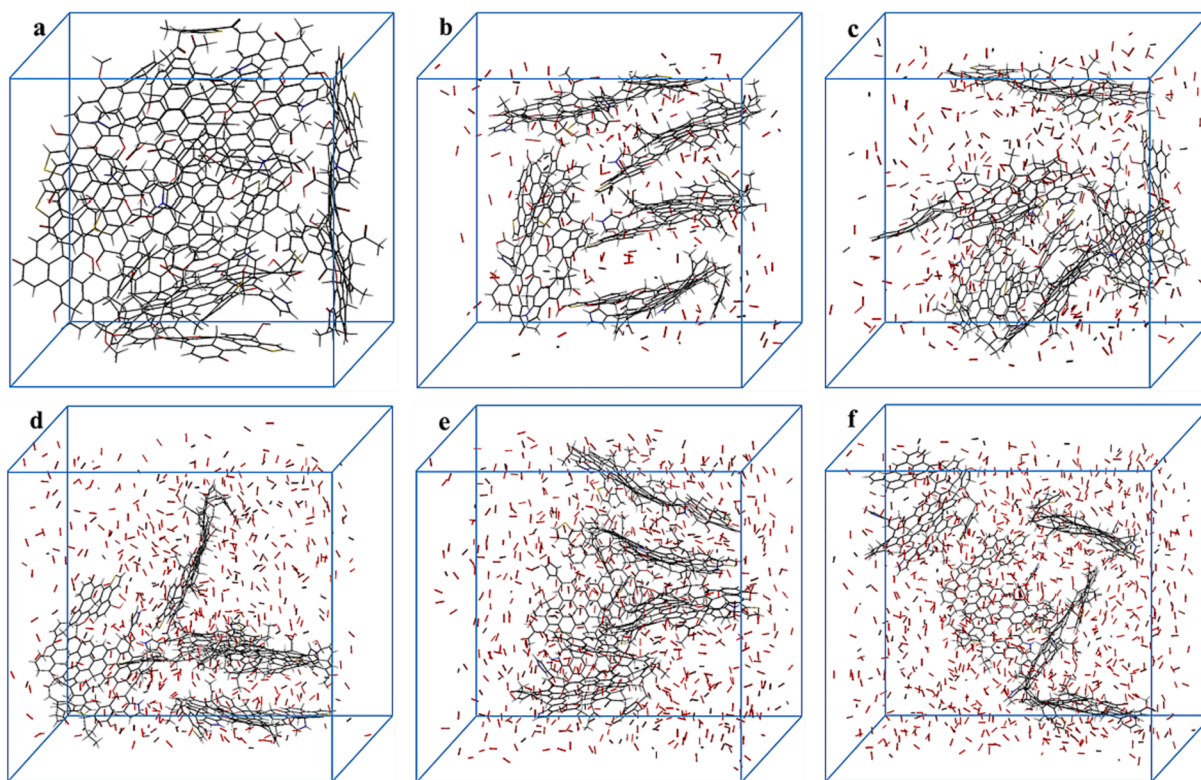


Fig. 8. KN coal reaction systems with different oxygen content.

3.5. Coal oxidation characteristics analysis

3.5.1. Enclosed coal oxidation test results

The air leakage rate in the loose coal bed inside the enclosed coal oxidation test setup can be regarded as a constant. Thus, according to mass transfer principles, the oxygen consumption rate λ_1 , and CO and CO₂ generation rates λ_2 and λ_3 at the same temperature under different oxygen volume fractions can be expressed as:

$$\lambda_1 = -\frac{df_1(C_1(\tau))}{d\tau} \cdot \frac{1}{22400} \quad (3)$$

$$\lambda_2 = -\frac{df_2(C_2(\tau))}{d\tau} \cdot \frac{1}{22400} \quad (4)$$

$$\lambda_3 = -\frac{df_3(C_3(\tau))}{d\tau} \cdot \frac{1}{22400} \quad (5)$$

Where $f_1(C_1(\tau))$, $f_2(C_2(\tau))$, $f_3(C_3(\tau))$ are functions corresponding to O₂, CO and CO₂ volume fractions in the enclosed coal oxidation tests, respectively; $C_1(\tau)$, $C_2(\tau)$, $C_3(\tau)$ represent O₂, CO and CO₂ volume fractions at time τ , %; λ_1 is the volumetric oxygen consumption rate, mol·(cm³·s)⁻¹; λ_2 is the CO volumetric release rate, mol·(cm³·s)⁻¹; λ_3 is the CO₂ volumetric release rate, mol·(cm³·s)⁻¹. τ is time, s.

The maximum temperature in the enclosed oxidation experiments is 70 °C. Hence, it can be assumed that oxygen is only converted to CO and CO₂ during the coal oxidation reactions inside the test setup, without considering other intermediates. The oxidation heat release intensity of coal can then be estimated using the bond energy balance method (Li et al., 2023; Chen et al., 2005; Chu et al., 2008):

$$Q = (\lambda_1 - \lambda_2 - \lambda_3)\Delta h_1 + \lambda_2\Delta h_2 + \lambda_3\Delta h_3 \quad (6)$$

Where Q is the oxidation heat release intensity, J·(cm³·s)⁻¹; Δh_1 is the chemical adsorption heat of coal oxidation, 58.80 KJ·mol⁻¹; Δh_2 is the heat for CO formation, 110.54 KJ·mol⁻¹; Δh_3 is the heat for CO₂ formation, 393.51 KJ·mol⁻¹.

Combining Equations 3–6, the oxygen consumption rate, CO and CO₂ generation rates, and oxidation heat release intensity of the coal samples under 20 % oxygen volume fraction at different temperatures were calculated and plotted in Fig. 7.

Fig. 7a and 7b show the variation of the three gases with time during the enclosed oxidation test at 25 °C. Fig. 7c-f illustrate that the oxygen consumption rate, CO and CO₂ generation rates, and oxidation heat release intensity of the coal sample all increase exponentially with rising temperature. Compared to 25 °C, the oxygen consumption rate, oxidation heat release intensity at 70 °C are enhanced by about 800 % and 700 %, respectively.

3.5.2. ReaxFF pyrolysis simulation of coal macromolecules

The enclosed coal oxidation experiments in this study focused on investigating the oxidation characteristics below 70 °C. ReaxFF simulation of coal has significant advantages in studying the chemical reactions, intermolecular interactions, structural evolution and product formation during coal high temperature reactions and combustion from the atomic level. The constructed mixed systems containing coal molecules and O₂ with different oxygen amounts are shown in Fig. 8. Assuming that all atoms in the coal molecule react completely to form stable structures (CO₂, H₂O, N₂, SO₂) through pyrolysis (Zhang, 2022). In this case, the number of oxygen molecules that need to be added to the reaction system is approximately 900, and the oxygen content of this reaction system is defined as 100 %. Therefore, the oxygen contents in Fig. 8 are sequentially: 0 %, 25 %, 50 %, 75 %, 100 %, and 125 %.

Fig. 9 illustrates the generation behaviors of indicator gases during the ReaxFF pyrolysis kinetics simulation of the KN coal sample, where Fig. 9a and 9b present the CO₂ and CO content changes along the reaction process. With increasing oxygen content in the reaction systems, the CO₂ and CO amounts also gradually rise. However, in the later reaction stage (250000 simulation steps), the CO content starts to decline while CO₂ increases, consistent with the trend exhibited in Fig. 7b. As displayed in Fig. 9c and 9d, the existence durations of C₂H₂ and C₂H₄ increase with higher oxygen content, and their content variation trends

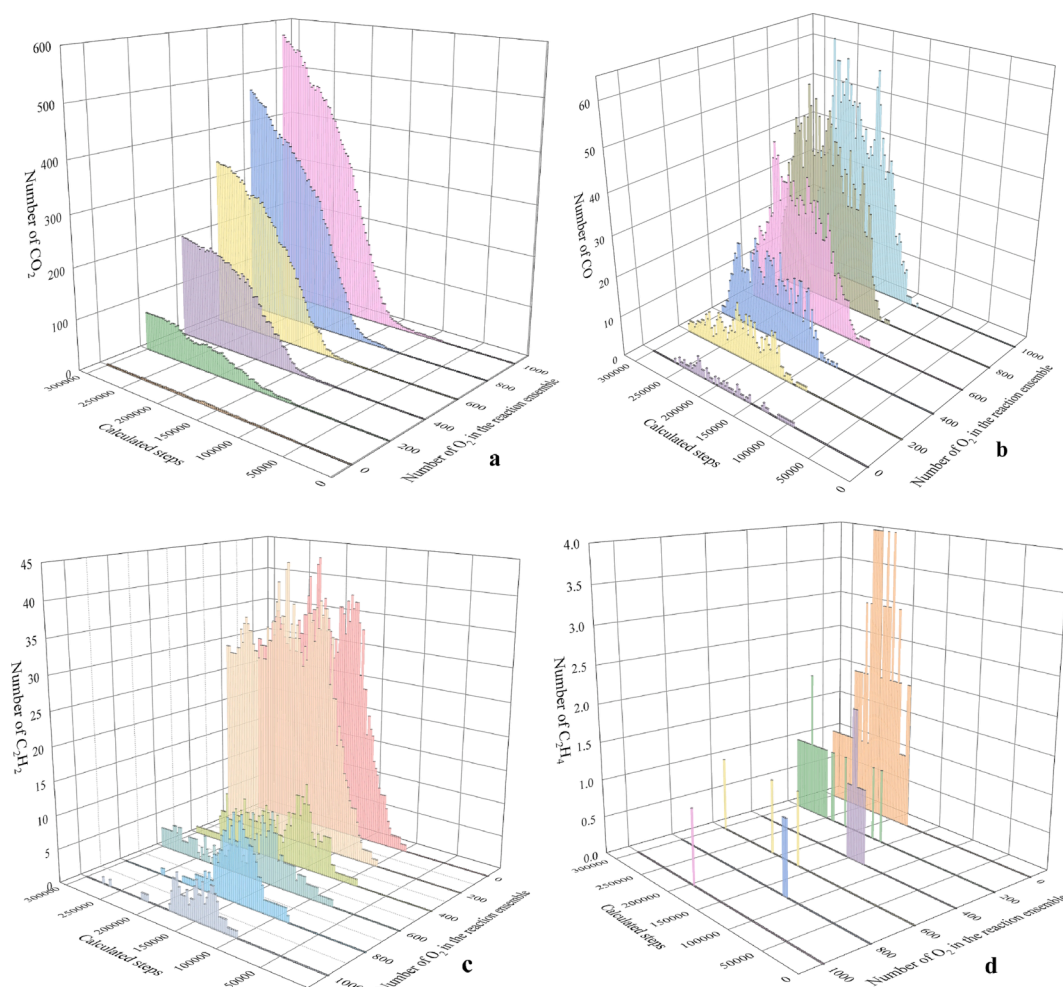


Fig. 9. Simulated generation patterns of indicator gases for KN coal sample.

are similar.

In the reaction system with 1000 oxygen molecules, the CO_2 , CO, C_2H_2 and C_2H_4 gas molecules were labeled and traced back to determine the initial positions of atoms in coal macromolecules that generate these four indicator gases. This allows identification of structural units in the KN coal molecule responsible for the oxidative formation of CO_2 , CO, C_2H_2 and C_2H_4 , thereby inferring their potential major reaction pathways, as depicted in Fig. 10.

The main generation pathways of CO_2 include:

(1) The C–H bond in the aldehyde is first broken to generate an aldehyde free radical, which then reacts with the oxygen molecule in the air to form an oxidized intermediate product, and finally CO_2 is generated through a series of reaction steps (including generation of ketone intermediates). (2) The carbon-hydrogen bond (C–H bond) in the phenol is broken to form a phenol free radical or ion. The phenol free radical reacts with the oxygen molecule in the air to generate an aldehyde and water. The generated aldehyde continues to oxidize and eventually forms carbon dioxide. (3) Carboxyl generation of CO_2 reaction process: the carboxyl group connected to the aromatic structure removes a hydrogen radical, and then detaches from the aromatic structure to form CO_2 . (4) Methoxy ($\text{CH}_3\text{O}\bullet$) reacts with oxygen to produce formaldehyde (CH_2O) and a hydrogen peroxide free radical ($\text{HO}_2\bullet$). Formaldehyde (CH_2O) is further oxidized to CO_2 and H_2O .

The main generation pathways of CO include:

(1) The hydrolysis reaction of esters generates carboxyl groups, followed by decarboxylation of carboxylic acids to generate CO. (2) Phenols undergo oxidative decarboxylation reactions to generate CO. (3)

Carbonyl compounds generate CO by breaking the carbon–oxygen double bond in the carbonyl. (4) Ethers directly thermally decompose to generate carbon-centered free radicals and CO.

The main generation pathways of C_2H_4 include:

(1) In structures connected to other structures, the cyclic alkane structure opens the ring and loses two connected carbon-containing structures that are not connected to other structures, which directly form a double bond to form a C_2H_4 molecule. (2) Alcohols undergo dehydration to generate carbocations. The carbocations are deprotonated to generate carbanions. Two carbanions are coupled to generate ethylene.

The main generation pathways of C_2H_2 include:

(1) In cyclic alkane structures connected to other structures, two connected carbon-containing structures that are not connected to other structures are released after ring opening, and then each carbon atom loses a hydrogen radical to form a carbon–carbon triple bond and form C_2H_2 . (2) In the structure where the benzene ring and cyclic alkane are connected, the cyclic alkane is broken, and the carbon atom on the cyclic alkane connecting the ethyl group is released along with the ethyl group. After the released part loses a methyl group as a whole, the remaining part forms a carbon–carbon triple bond to form a C_2H_2 molecule.

4. Conclusions

This study used experimental and computational simulation methods to characterize the oxidation characteristics and generation laws of indicator gases of Kunming coal from macroscopic and microscopic

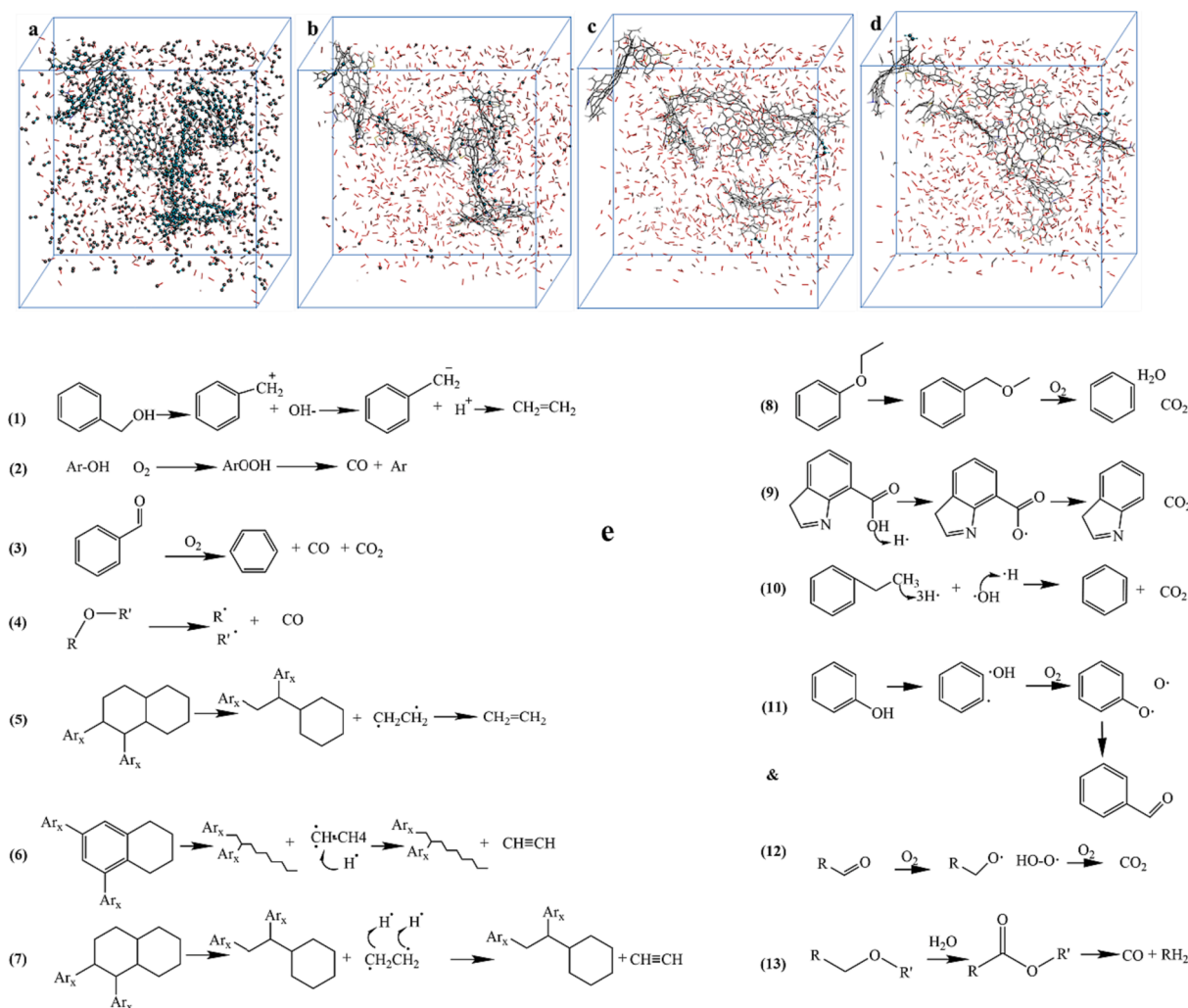


Fig. 10. Positions and reaction pathways of indicator gas molecules generated from KN coal.

perspectives, and obtained the following main conclusions:

- (1) The ratio of bridging carbon to peripheral carbon X_{BP} in the coal molecular structure is 0.08. The aromatic compounds in the KN coal sample consist mainly of benzene and naphthalene ring structures. Oxygen atoms exist in the form of carbonyl, hydroxyl and ether bonds, and nitrogen and sulfur atoms exist in the form of pyrrole and thiophene, respectively. The finally constructed single molecular structure formula of KN coal is $C_{149}H_{76}O_{15}N_2S_2$.
- (2) The curve of oxygen volume fraction change over time obtained from the closed coal oxidation test follows an exponential decay distribution. The final steady-state value of oxygen volume fraction of KunNing coal sample is around 6 % at room temperature. As the test temperature increases, the oxygen consumption rate, CO release rate, CO₂ release rate and oxidation heat release intensity of coal increase exponentially.
- (3) Molecular reaction dynamics simulations using the ReaxFF force field show that the yields of CO and CO₂ are positively correlated with the number of oxygen molecules in the reaction system, while C₂H₂ and C₂H₄ are negatively correlated. CO₂ mainly comes from aldehydes, phenols, carboxyls and methoxys in coal molecules, CO is mainly generated from esters, phenols, carbonyls, etc., C₂H₂ is mainly derived from the ring opening and breaking of cyclic alkanes, and C₂H₄ generation is mainly related to cyclic alkanes and alcohols.

CRediT authorship contribution statement

Dongjie Hu: Supervision, Funding acquisition. **Zongxiang Li:** Data curation. **Yu Liu:** Supervision. **Lin Li:** Data curation, Supervision.

Acknowledgments

The authors acknowledge the financial support from the National Natural Science Foundation of China (51774170).

References

- Bhoi, S., Banerjee, T., Mohanty, K., 2014. Molecular dynamic simulation of spontaneous combustion and pyrolysis of brown coal using Reax FF. *Fuel* 136, 326–333.
- Chen, X.K., Yi, X., Deng, J., 2005. Experiment study of characteristic self-heating intensity of coal [J]. *Journal of China Coal Society* 30 (5), 81–84.
- Chu, T.X., Yang, S.Q., Sun, Y., Sun, J.K., Liu, Z.P., 2008. Experimental study on low temperature oxidation of coal and its infrared spectrum analysis [J]. *China Safety Science Journal* 18 (1), 171–177.
- Ding, C., Li, Z.X., Hu, D.J., Gao, D.M., 2023. Construction of macromolecular model and analysis of oxygen absorption characteristics of Hongyang No. 2 coal mine [J]. *Arab. J. Chem.* 16 (5), 104662.
- Feng, W., Gao, H., Liu, T., 2019. ReaxFF Molecular Dynamics Simulations of the Combustion Reactions of Pyrrole and Pyridine [J]. *Acta Petroli Sinica (petroleum Processing Section)* 35 (6), 1130–1137.
- Gao, D.M., 2021. Research on Gas Chemical Generating Mechanism in the Process of Coal and Gas Outburst [D]. Liaoning Technical University.
- Gao, M., Li, X., Guo, L., 2018. Pyrolysis simulations of Fugu coal by large-scale ReaxFF molecular dynamics [J]. *Fuel Process. Technol.* 178, 197–205.

- Given, P.H., 1959. Structure of bituminous coals: evidence from distribution of hydrogen. *Nature* 184, 980–981.
- Hu, D.J., Li, Z.X., 2022. Dynamic distribution and prevention of spontaneous combustion of coal in gob-side entry retaining goaf[J]. *PLoS One* 17 (5), e0267631.
- Jiang, Y., Zong, P.J., Tian, B., Xu, F., Tian, Y., 2019. Pyrolysis behaviors and product distribution of Shenmu coal at high heating rate: A study using TG-FTIR and Py-GC/MS. *Energ. Convers. Manage.* 179, 72–80.
- Li, Z.X., Liu, Y., Wu, B.D., Zhang, H.B., Jia, J.Z., 2017. Critical oxygen volume fraction of smothering quenched zone based on closed oxygen consumption experiment [J]. *J. China Coal Soc.* 42 (7), 1776–1781.
- Li, Z.X., Zhang, M.Q., Yang, Z.B., Liu, Y., Ding, C., 2023. Effect of fault structure on the structure and oxidative spontaneous combustion characteristics of coal [J]. *J. China Coal Soc.* 48 (3), 1246–1254.
- Liang, Y.T., Hou, X.J., Luo, H.Z., Tian, F.C., Yu, G.S., 2016. Development countermeasures and current situation of coal mine fire prevention & extinguishing in China. *Coal Science and Technology.* 44–6, 1–6+13.
- Liu, Q., 2019. Study of the occurrence of sulfur in coal from Huainan-HuaiBei areas and its migration characteristics in pyrolysis [D]. *Anhui University of Technology.*
- Y. Liu, F. S. Wang, X. M. Dong, D. Gao. Study on the Characteristics and Microscopic Mechanism of Coal Spontaneous Combustion Based on Programmed Heating Experiment [J/OL]. *Coal Science and Technology*:1-13.
- Long, H., Lin, H., Yan, M., Bai, Y., Xiao, X., Kong, X.G., Li, S.G., 2021. Adsorption and diffusion characteristics of CH₄, CO₂, and N₂ in micropores and mesopores of bituminous coal: Molecular dynamics[J]. *Fuel* 292, 120268.
- Mathews, J.P., Duin, A.C.T.V., Chaffee, A.L., 2011. The utility of coal molecular models. *Fuel Process. Technol.* 92 (4), 718–728.
- J. Q. Meng, R. Q. Zhong, S. C. Li, F. F. Yin, B. S. Nie. Molecular model construction and study of gas adsorption of Zhaozhuang coal. *Energy & Fuels*, 2018, 32(9): 9727-9737.
- Onifade, M., Genc, B., 2020. A review of research on spontaneous combustion of coal. *Int. J. Min. Sci. Technol.* 30–3, 303–311.
- Sen, K., Dash, P.S., 2020. Quantum chemical perspective of coal molecular modeling: A review [J]. *Fuel* 279, 118539.
- Shinn, J.H., 1996. Visualization of complex hydrocarbon reaction systems. *Preprints of Papers American Chemical Society Division of Fuel Chemistry* 41 (6), 418.
- Solum, M.S., Pugmire, R.J., Grant, D.M., 1989. Carbon-13 solid-state NMR of Argonne-premium coals [J]. *Energy Fuel* 3 (2), 187–193.
- Trewhella, M.J., Popletti, J.F., Grint, A., 1986. Structure of green river oil shale kerogen: Determination using solid state ¹³C NMR Spectroscopy. *Fuel* 65 (4), 541–546.
- Wiser, W.H., 1984. Conversion of bituminous coal to liquids and gases: chemistry and representative processes. *Magnetic Resonance*. Springer, Netherlands.
- Yao, M.Y., Liu, Y.H., Che, D.F., 2003. Investigation of nitrogen functionality in Yibin coal and its change laws. *Journal of xi'an Jiaotong University* 37 (7), 759–763.
- Zeng, Q., Pu, Y., Cao, Z.M., 2018. Kinetics of oxidation and spontaneous combustion of major super-thick coal seam in Eastern Junggar Coalfield, Xinjiang, China. *J. Loss Prev. Process Ind.* 56, 128–136.
- Zhan, J.H., Wu, R., Liu, X.X., Gao, S.Q., Xu, G.W., 2014. Preliminary understanding of initial reaction process for subbituminous coal pyrolysis with molecular dynamics simulation [J]. *Fuel* 134, 283–292.
- Zhang, J., 2022. Generation and Adsorption Mechanism of Coal Spontaneous Combustion Index Gases and Goaf Dangerous Zones Classification Division [D]. *Liaoning Technical University.*
- Zhang, J.F., Clennell, M.B., Dewhurst, D.N., Liu, K.Y., 2014. Combined Monte Carlo and molecular dynamics simulation of methane adsorption on dry and moist coal[J]. *Fuel* 122, 186–197.
- Zhang, Y.T., Li, Y.Q., Deng, J., Zhang, X.H., 2015. Study on catastrophe characteristics of coal spontaneous combustion. *China Safety Science Journal.* 25–1, 78–84.
- Zheng, M., Li, X.X., Liu, J., Guo, L., 2013. Initial chemical reaction simulation of coal pyrolysis via ReaxFF molecular dynamics[J]. *Energy Fuel* 27 (6), 2942–2951.
- Zhou, Q., 2008. Study on occurrence mode of sulfur and nitrogen in coal in China [J]. *Clean Coal Technology* 53 (1), 73–77.